ROYAL SOCIETY
OF CHEMISTRY

PAPER

Check for updates

A single molecule stimuli-robust fluorescent hydrogel based on excited state intramolecular proton transfer

Ankur A. Awasthi,[ab] Luís Gustavo Teixeira Alves Duarte, [ID] †*[c]
Fabiano Severo Rodembusch, [ID] [d] Teresa Dib Zambon Atvars [ID] [c] and
Cornelia Bohne [ID] *[ab]

A white light-emitting hydrogel was synthesized by embedding *N,N'*-bis(salicylidene)-(2-(3',4'-diaminophenyl)benzothiazole) (BTS) into a polyethylene oxide–polypropylene oxide–polyethylene oxide (PEO–PPO–PEO, F127) triblock copolymer hydrogel. BTS undergoes excited state intramolecular proton transfer (ESIPT), which leads to a broad emission spectrum where both the normal (N*) and tautomeric (T*) forms of the excited states of BTS coexist. Aggregation of BTS was prevented when it was embedded in F127 hydrogels. The BTS emission spectra are sensitive to the BTS loading in the gel, with white light being observed for some concentrations of lumiphore. In contrast, the BTS emission spectra are insensitive to pH. These experiments showed the successful application of a supramolecular strategy where the lumiphore is incorporated into a specific environment in the micelles forming the gel. The insensitivity of the emission colour to pH showed that emissive materials using a single ESIPT molecule can be achieved without the pH sensitivity normally associated with this process. These results highlight the importance of designing fluorophores with properties that enable them to be located in specific environments of supramolecular systems.

Introduction

Hydrogels are soft and viscoelastic materials containing entrapped water within an immobile gel phase. Hydrogels have found applications in various fields such as in bioengineering,[1] food and cosmetics industries,[2,3] oil exploration,[4,5] or as functional materials.[6] Examples of functional materials are drug delivery systems,[7] sensors,[8,9] organic field emitting transistors,[10,11] hydrogen production[12,13] and luminescent hydrogels.[14,15] Luminescent hydrogels have exhibited potential for applications in chemical and biosensing,[16–18] imaging,[19,20] anti-counterfeiting[15,21] and in the fabrication of displays.[22]

Different approaches are used for the development of luminescent hydrogels. In a synthetic approach, the gelator is synthetically modified to attain the desired luminescent properties.[23] In a supramolecular approach, lumiphores are incorporated as non-bonded guests within the hydrogel.[14] The incorporation of metal ions and their complexes,[15,24] dyes,[25,26] quantum dots[27,28] or carbon dots[29,30] was used for the development of luminescent hydrogels, showing that luminescent properties in hydrogels can be tuned without requiring a tailored synthetic effort for each desired modification.

A major motivation behind obtaining luminescent materials is to achieve white light emitting hydrogels as a desirable property for a variety of applications such as wearable optoelectronic devices,[31] environmental sensors,[21] biosensors,[17,18] and bioimaging modalities.[22] White light can be obtained by integrating into a hydrogel three fluorophores each with emissions corresponding to one of the three primary colours,[32,33] or by integrating two fluorophores with emissions that have complementary colours.[22] In both strategies the colour of the emitted light is controlled by the concentration ratio between the fluorophores.[32,33] These strategies were successful with the integration of fluorophores into hydrogels either through the fluorophore's covalent binding to the gelator,[34,35] coordination to the gel matrix,[31] or physical entrapment within the gel.[15,16,36]

[a] *Department of Chemistry, University of Victoria, PO Box 1700 STNCSC, Victoria, BC, V8W 2Y2, Canada. E-mail: ankur.a.awasthi@gmail.com, bohne@uvic.ca, cornelia.bohne@gmail.com*

[b] *Centre for Advanced Materials and Related Technology (CAMTEC), University of Victoria, 3800 Finnerty Rd, Victoria, BC, V8P 5C2, Canada*

[c] *Chemistry Institute, University of Campinas, PO Box 6154, Campinas, Brazil. E-mail: lduarte@iciq.es, lg.alvesduarte@gmail.com, tatvars@unicamp.br*

[d] *Grupo de Pesquisa em Fotoquímica Orgânica Aplicada, Universidade Federal do Rio Grande do Sul, Porto Alegre, Brazil. E-mail: rodembusch@iq.ufrgs.br*

† Present address: Institute of Chemical Research of Catalonia (ICIQ-CERCA), Barcelona Institute of Science and Technology (BIST), Avda. Països Catalans 16, Tarragona 43007, Spain.

However, the use of multiple fluorophores can lead to unpredictable changes in the fluorescence properties of the gel, especially when the distribution of the fluorophores between the immobile and aqueous phases of the gel changes. In contrast, luminescent materials based on the use of a single molecule, which can reversibly form other emitting species, avoids the use of multiple fluorophores to achieve different colours of light. Examples of this single molecule approach are the copolymerization of a fluorophore with acrylamide,[37] or the modulation of the acid–base equilibrium of a fluorophore in the ground state within the gel.[36]

Our objective was to develop a white light emitting hydrogel where primarily one ground state species of a fluorophore exists in a specific environment of the hydrogel. In contrast to ground state molecules, singlet excited states of organic fluorophores are short lived, precluding any relocation of these excited states between the different environments of supramolecular systems,[38,39] such as gels. An additional objective was to test for the robustness of using a hydrogel to disperse a fluorophore. To address this, we chose a fluorophore that has shown multiple emissions on account of proton transfer reactions in both ground and excited states.[40] The design of our system (Fig. 1) relies on the excited state intramolecular proton transfer (ESIPT) of N,N′-bis(salicylidene)-(2-(3′,4′-diaminophenyl)benzothiazole) (BTS) when incorporated into the hydrogel formed from a polyethylene oxide–polypropylene oxide–polyethylene oxide (PEO–PPO–PEO, F127) triblock copolymer.

In ESIPT, the singlet excited state tautomer (T*) is formed from the intramolecular proton transfer of the excited isomer (N*) that is the only stable isomer in the ground state (N) (Fig. 1a).[41,42] Once T* decays to its ground state, the isomer T is readily converted to N in a ground state intramolecular proton transfer (GSIPT) process.[41–44] This four-level system ensures that only N is prevalent in the ground state, while in the excited state N* and T* coexist leading to a broadening of the overall emission spectrum as both N* and T* emit.

BTS was chosen as the fluorophore because it undergoes ESIPT and white light was obtained when BTS was dispersed in the polymeric matrix of an organic light emitting diode (OLED) because of the simultaneous emissions from the normal (N*) and tautomeric (T*) forms of the chromophore.[40,45] However, the emission spectra of the OLED were dependent on the concentration of BTS likely due to aggregation of the
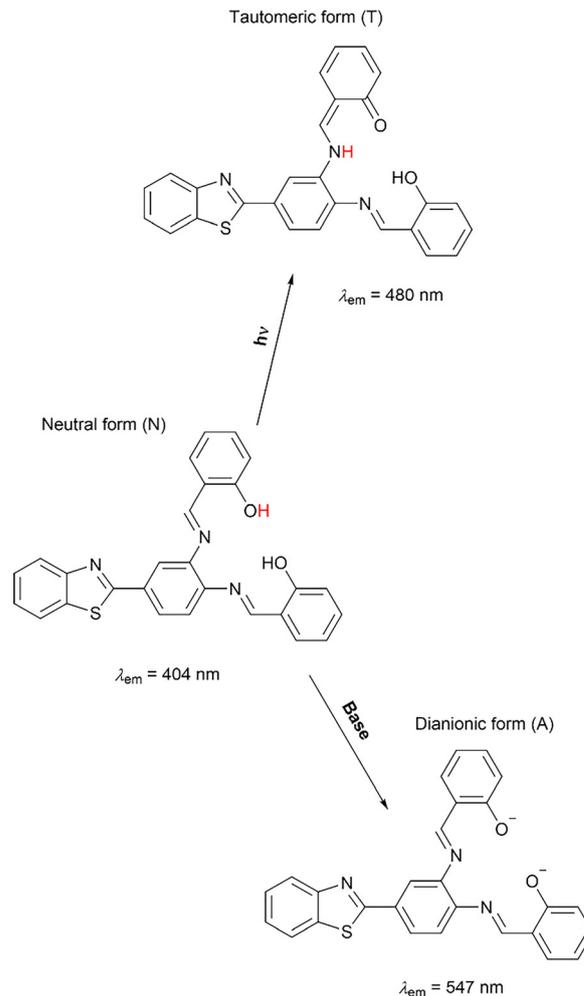
Scheme 1 Isomers of BTS and its dianion with their reported emission maxima in dichloromethane.[40]

fluorophore. In addition, BTS in dilute solutions deprotonates and forms a dianion (A) in the ground state, which emits at a longer wavelength than T* (Scheme 1).[40,46] The presence of the dianion is not desired in a strictly single molecule approach. However, in our design the presence of A was used to test for the robustness of the colour emitted to changes in pH.

Pluronic F127 was chosen because this triblock copolymer forms a clear and thermosensitive gel.[47,48] These are important
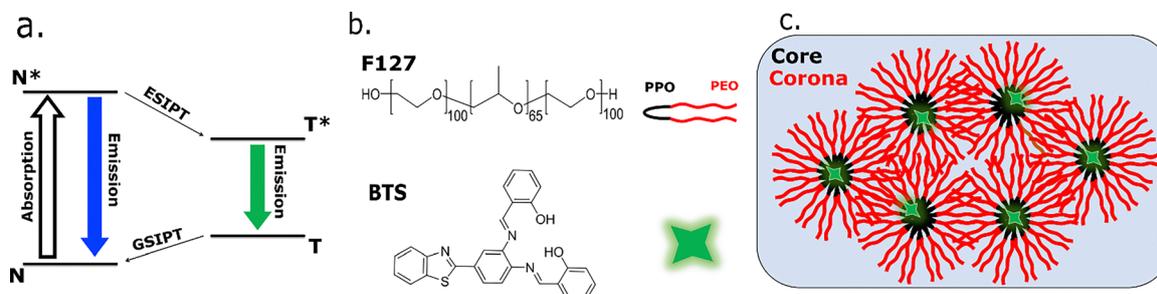

Fig. 1 (a) Four-level-diagram of the ESIPT process (b) structures of F127 and BTS (c) cartoon representation of the F127 hydrogel with BTS.

properties for luminescent materials and for the manufacture of devices. There is precedent for the observation of white light in a F127 hydrogel when the neutral form of a fluorophore and its conjugated acid are located respectively in the micellar core and the gel's aqueous phase.[36] Pluronics form micelles upon heating because the PPO segments are preferentially dehydrated forming the micellar core, which is surrounded by the PEO chains in the corona (Fig. 1c).[47,49] At high F127 concentrations and further heating, the aqueous micellar solution forms a gel because of the entanglements of the PEO chains.[47,49] This gel has three microenvironments, the bulk water, corona and hydrophobic core (Fig. 1c) that have different properties.[50,51] BTS as a hydrophobic and water insoluble fluorophore is expected to be solubilized in the PPO micellar core, as was shown to be the case for other hydrophobic molecules.[50–52]

Experimental

Materials

Pluronic F127 (Sigma-Aldrich, M_W = 12 600 Da, 70 wt% PEO) and dichloromethane (DCM, Fischer, HPLC grade >99.8%) were used as received. Deionized water (Branstead NANOpure deionizing system ≥17.8 MΩ cm) was used for the preparation of all aqueous solutions. BTS was synthesized and purified as previously reported (Fig. S1).[40]

Methods

Sample preparation

All hydrogel samples were made using 17% (w/w) F127 by adding 4.0 g of F127 to 20 mL of water in an ice bath while stirring until all solid F127 dissolved. For solutions prepared at different pH values, the pH of water was first adjusted using HCl or NaOH to obtain the desired pH value and this water was then used to prepare the 17% (w/w) F127 samples.

BTS was solubilized in DCM yielding an 800 μM stock solution. An aliquot of BTS in DCM was added to a glass vial, after which DCM was evaporated under a gentle air flow. After DCM evaporation, 4 mL of the 17% (w/w) F127 solution was added to the vial. This solution was then stirred for a week in an ice bath to ensure complete dissolution of BTS into 17% (w/w) F127. After a week, 3 mL of this BTS/F127 solution was transferred to a 10 mm × 10 mm quartz cell to carry out the photophysical studies. The low solubility of BTS in water precluded the determination of the BTS molar absorptivity in this solvent. For this reason, concentrations of BTS are indicated as the absorption value measured at 335 nm (A_{335}).

Instrumentation

^{1}H NMR spectra were acquired using DMSO-d_6 as the solvent on a Varian 400 MHz or a Bruker 400 MHz spectrometer. A VWR SympHony B10P pH meter was used to measure the pH of the solutions.

Absorption spectra were collected on a CARY 100 Varian spectrometer at a scan rate of 600 nm min^{-1}. Emission spectra were measured using a PTI QM-40 spectrofluorimeter using slits corresponding to 2.0 nm bandwidths for the excitation and emission monochromators. Samples were excited between 340 and 480 nm. The colour of the emission from the gel was determined from the fluorescence spectra collected in two wavelength ranges with a 20 nm gap centred at double the excitation wavelength. This gap is required to avoid detection of excitation light. A linear dependence was assumed between the two wavelengths defining the gap. The emission of a control sample containing the F127 gel but not the fluorophore was subtracted from the BTS/gel spectrum to correct for the emission from the F127 sample and any light scattering (Fig. S2 and S3). The Colour Calculator from Osram Sylvania was used to obtain chromaticity diagrams and to determine the Commission Internationale de l'Eclairage (CIE 1931) coordinates of chromaticity.

Time-resolved emission decays were collected using an Edinburgh Instruments OB920 single photon counting system. A light emitting diode was used to excite the samples at 335 nm (EPLED-330, Edinburgh Instruments) and the emission was collected at specific wavelengths using a monochromator bandwidth of 16 nm. The instrument response function (IRF) was collected using an aqueous Ludox solution which scattered the excitation light. The data were collected until the highest intensity in the collecting channels reached 5000 counts. The time-resolved decays were fit to a sum of exponentials (eqn (1)) using the software provided by Edinburgh Instruments, where A_i corresponds to the pre-exponential factor of species "i" and τ_i corresponds to the lifetime of species "i". The sum of the A_i values is equal to unity. To account for the IRF, a re-convolution of the IRF with the calculated decay was performed during the fitting of the experimental data.

$$I(t) = I_o \sum_1^i A_i e^{-\frac{t}{\tau_i}} \qquad (1)$$

The goodness of the fit was judged by the χ^2 value recovered from the fit and by the visual inspection of the residuals. Fits with χ^2 values between 0.9 and 1.2 and having a random distribution of residuals around zero between the experimental and calculated values were deemed adequate.[53]

Results and discussion

Incorporation of BTS into F127 avoids the aggregation previously observed when BTS was dispersed in an OLED layer,[40] and the colour for the emission of BTS in F127 is similar when F127 is in the sol (20 °C) or gel phases (30 °C). The absorption spectrum of A ($\lambda_{\max}$ = 430 nm) is red shifted with respect to the spectrum of N, and these species cannot be excited separately since their absorption spectra overlap. The absorption spectra of BTS are the same in the F127 sol or gel phases (inset Fig. 2). Therefore, any changes in the emission spectra in the sol and gel phases are a result of the excited state properties of the BTS species (N*, T* and A*) in each phase and are not due to different ratios of species (N vs. A) in the ground state. N is primarily excited at 340 nm, leading to the emission from N* and T*, while a significant contribution of the emission from
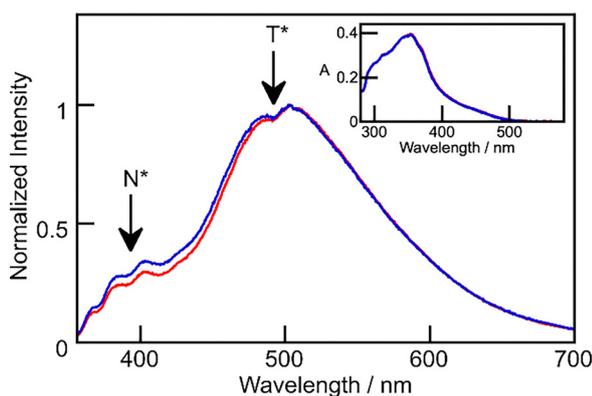
Fig. 2 Normalized steady-state emission spectra (λ_{ex} = 340 nm) of BTS (A_{335} = 0.4; absorbance values were used as a proxy for concentrations – see the Experimental section) in 17% (w/w) F127 at 20 °C (red, sol) and 30 °C (blue, gel). Inset: Absorption spectra of BTS in 17% (w/w) F127 at 20 °C (red, sol) and 30 °C (blue, gel).

A*, if present, is achieved when the sample is excited at longer wavelengths ($\lambda_{ex} \geq$ 400 nm).[40] The N* emission (λ_{ex} = 340 nm) is observed in the 400 nm region, while the T* emission is centred around 500 nm (Fig. 2). For the N* emission, shoulders were observed at 360, 380 and 396 nm, while for T* a shoulder and a peak were seen at 480 and 500 nm, respectively. These features are different from the emission spectra for BTS in solution and when dispersed in a polymer.[40] No shoulders were observed for the emission of N* and T* in solution.[40] In the polymer, most of the emission arises from T* and the emission maximum occurs at a longer wavelength (563 nm) than observed in F127. The longer emission wavelength in the polymer was proposed to be due to the presence of aggregates of BTS.[40] The different photophysics of BTS in the gel and in the polymer suggests that the environment provided by the F127 micelles inhibits the aggregation of BTS molecules. The observation of similar emission spectra of BTS in the sol and gel phases shows that the colour of the emitted light does not depend on the phase of the system.

Experiments at incremental excitation wavelengths led to the observation of the emission from A* (Fig. 3 and Fig. S4). The absorption spectra of N* and A* overlap. For this reason, the emission of N*, T*, formed by ESIPT, and A* can occur for excitation wavelengths where N and A are excited. The relative intensities for the emission from these three species depends on the excitation wavelength with a higher contribution of the emission from A* occurring at longer excitation wavelengths.[40] The emission from N* around 400 nm was observed when the gel was excited at 340 nm, while the emission spectrum for excitation at 410 nm corresponds to a combination of the emission spectra for T* and A*. For excitation wavelengths above 450 nm, the emission spectrum predominantly corresponds to the emission of A*. These spectral assignments are supported by excitation spectra collected at different emission wavelengths, where the emission of A* at 600 nm led to a peak in the excitation spectrum around 460 nm consistent with the previous characterization of A (Fig. 3).[40] An
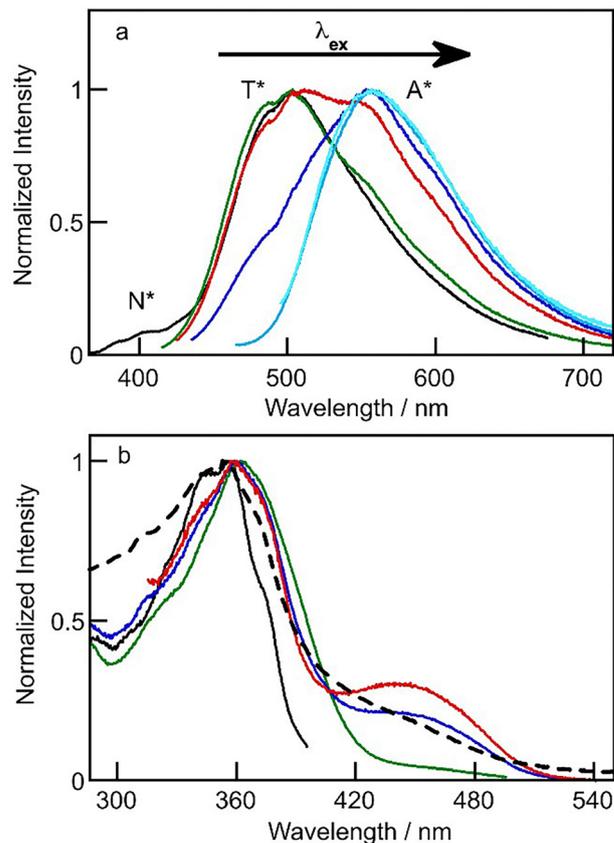

Fig. 3 (a) Normalised steady-state emission spectra of BTS in 17% (w/w) F127 at 30 °C for different excitation wavelengths: 340 nm (black), 400 nm (green), 410 nm (red), 420 nm (dark blue), 450 nm (blue) and 480 nm (light blue). (b) Normalized excitation spectra of BTS in 17% (w/w) F127 at 30 °C monitored at different emission wavelengths: 400 nm (black), 500 nm (green), 550 nm (blue) and 600 nm (red). The dashed line represents the absorption spectrum.

excited-state double proton transfer (ESDPT) process[54] was considered for the BTS emission because of the presence of two phenolic hydrogens, but this mechanism is inconsistent with the experimental data. For ESDPT, the two emissions at longer wavelength would correspond to the mono- and di-tautomeric excited states formed from N*. The longest wavelength emission of BTS was previously observed in pyridine where BTS is deprotonated and excited-state proton transfer is supressed.[40] The profiles for the excitation and emission wavelengths of BTS in the F27 gel are consistent with the studies in pyridine and indicate that two different species are present in the ground state. In addition, for ESDPT the relative intensities of both the mono- and di-tautomeric emissions should have decreased at longer excitation wavelengths, which is opposite to the experimental observations. Therefore, the emission and excitation profiles of BTS in F127 gels showed that the emission of A* contributed to the definition of the colour of the emission of BTS in the gel.

The 1931 CIE chromaticity diagram, described by the National Bureau of Standards (NBS), was used to determine the colour of emission from the BTS/F127 hydrogels. In this
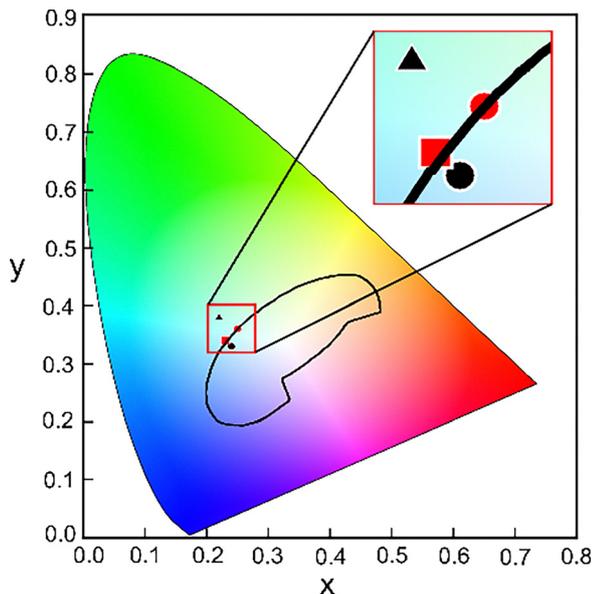
Fig. 4 Chromaticity diagram (x, hue and y, saturation) for the emission of BTS in 17% (w/w) F127 hydrogels with varying BTS concentrations, which were quantified as the BTS absorbance (A_{335} = 0.2 (●), A_{335} = 0.4 (●), A_{335} = 0.6 (■), which is covered by the A_{335} = 0.8 point (■), and A_{335} = 1.1 (▲)). Corresponding emission profiles of BTS are shown in Fig. 2 and Fig. S5–S8. The area defined by the black line corresponds to colours that are perceived as white.[55]

Fig. 5 Normalized steady-state emission spectra of BTS (λ_{exc} = 340 nm, inset: λ_{exc} = 400 nm) in 17% (w/w) F127 hydrogel at 30 °C at various pH values (pH 4 (black), pH 5 (red), pH 6 (blue), pH 7 (green), pH 8 (black)).

chromaticity diagram,[55] the colour of the emission is independent of the luminance, which means that the colour does not depend on the intensity of the emitted light. The colour of the BTS emission in the F127 gel changed with the BTS concentration (Fig. 4 and Fig. S5–S9, Table S1). As this concentration was raised, the colour of the emitted light moved toward the boundary of what is considered white light emission (Fig. 4).[55] At the highest concentration studied (A_{355} = 1.1), the colour of the emission became light blue with chromaticity coordinates outside the acceptable white light emission region. The colour shift observed is a consequence of the higher contribution of the emission from T* as the concentration of BTS increases, indicating that the colour of this system can be modulated by changing the BTS concentration. The increased contribution from T* could be related to the population of sites in the gel with slightly different properties or could be related to the onset of aggregation which in polymers was shown to influence the emission properties of BTS.[40]

The role of the dianionic form of BTS (A) on the emission of the BTS/F127 system was investigated by changing the pH, because the presence of A is sensitive to pH. The emission spectra for BTS/F127 hydrogels measured between the pH values of 4 and 8 showed small changes in the 530 to 600 nm region where A* emits (Fig. 5). These changes did not lead to a significant change in the colour of the emission from the gel (Fig. S10 and Table S2) and there were no defined trends with pH for the changes in the spectra. This insensitivity to the pH was observed when the gel was excited at 340 nm, where N is excited, and when the gel was excited at 400 nm, where a higher
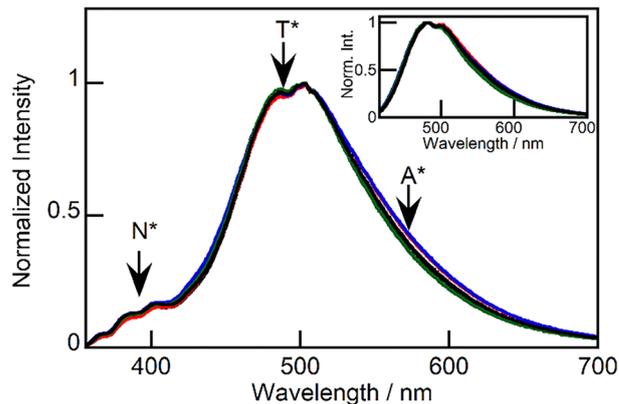
contribution of A* to the emission spectrum occurs. These results indicate that the pH does not change the ratio between the N and A concentrations, suggesting that BTS is in an environment in the F127 micelles that is shielded from the gel's aqueous phase leading to the insensitivity to pH of the relative amount of A present. The formation of the dianion likely occurs by proton abstraction from acceptor sites present in the F127 environment where BTS is located, a phenomenon previously observed for ESIPT-reactive systems in polymeric phases.[56]

Time-resolved fluorescence studies were used to obtain further insights into the photophysics of BTS in the F127 gel. The decays for samples excited at 335 nm were non-exponential and were faster when measured at 400 nm than those measured at 500 and 550 nm (Fig. 6). These results are consistent with the emission of BTS in DCM where non-exponential decays were observed with lifetimes of 08–0.9 and 2.8–2.9 ns for N*, 0.9 and 3.5 ns for T* and 0.4–1.0 and 3.2–3.6 ns for A*.[40] In the case of the BTS emission in the F127 gel, the lifetime of the emission from BTS overlapped with the emissions of F127 in the absence of BTS (Fig. S2 and S3). This low-level emission of F127 samples in the absence of BTS is likely due to impurities in F127 since its intensity depends on the F127 sample. However, low level emission from micellization seen for other polymeric micelles[57] cannot be ruled out. The emissions from F127 do not contribute significantly to the steady-state emission spectra of BTS (Fig. S2). However, in fluorescence decay measurements the emissions from F127 will be included in the overall decay despite the small amplitude for this emission compared to the overall emission (e.g. 2% for detection at 400 nm). The decays for the emission from F127 samples in the absence of BTS were adequately fit to a sum of three exponential terms (Fig. S11). The recovered lifetimes ranged between 0.1 and 10 ns (Table S3), which overlaps with the lifetime ranges of the BTS emission (Tables S4–S8). This overlap precludes a detailed analysis of the two BTS lifetimes observed in DCM and the analysis focussed on the longest-lived component for each BTS species (see the SI for details). At 400 nm, the wavelength for which the maximum contribution from N* is observed, the decay of BTS
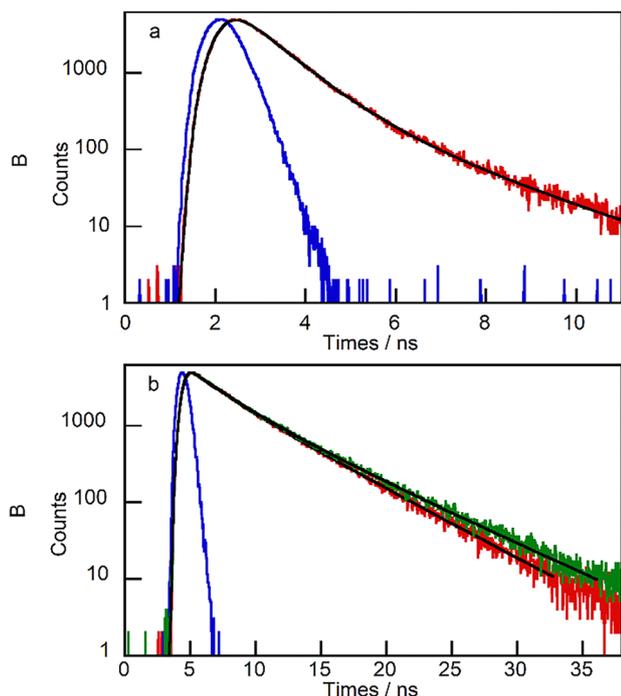
Fig. 6 Time-resolved decays for the singlet excited states of BTS (λ_{exc} = 335 nm) in 17% (w/w) F127 hydrogels at 30 °C. (a) λ_{em} = 400 nm (red) (b) λ_{em} = 500 nm (red), λ_{em} = 550 nm (green). The solid blue lines represent the IRFs, whereas the solid black lines represent the fits of the decays.

in the F127 gel was faster than at 500 nm, where the emission from T* is predominant, and at 550 nm where the contribution from A* is highest (Fig. 6). The lifetimes of T* and A* did not depend on the concentration of BTS and within experimental errors the lifetimes in the sol (6.2 ± 0.5 ns for T* and 3.3 ± 0.2 ns for A*) and gel phases (5.8 ± 0.3 ns for T* and 3.0 ± 0.3 ns for A*) are the same. The presence of N* and T* was confirmed by constructing time-resolved area-normalized emission spectra (TRANES),[58,59] which showed an isoemissive point, accompanied by the disappearance of N* and appearance of T* over time (Fig. S12) These results are consistent with previous time-resolved emission spectra for BTS in DCM,[40] showing that the gel did not alter the excited state reactivity of BTS (ESIPT).

The location of BTS in the F127 micelles defines the properties of the emission in the sol and the gel. BTS is not soluble in water and the compartmentalization afforded by the F127 micelles makes it possible to separate individual BTS molecules, while the system (sol or gel) is still in an aqueous environment. The photophysical properties in the gel are aligned with previous reports in solution and solid polymers,[40] and are supported by previous computational studies on the ESIPT process of BTS and related compounds.[40,45,60–62] The isolation of BTS molecules within the F127 micelles led to an emission at shorter wavelengths than observed for BTS incorporated into an OLED where aggregation occurred.[40,45] However, in both cases white light emission was achieved because of the presence of several emitting species.

BTS is incorporated into the core of F127 micelles since changes in pH did not affect the emission spectra of the BTS/ F127 gels. If BTS was partitioned between the hydrophobic core of the micelle and the PEO corona, the amount of deprotonated A would depend on the pH since the corona is exposed to the aqueous phase. Therefore, the BTS/F127 gel is an example where the fluorophore has multiple emissive species, one of which is pH sensitive, where the isolation of the fluorophore in one compartment of the system makes the emission resistant to changes in pH. This result contrasts with a previous study where the protonated fluorophore resided in the aqueous phase of the F127 gel while the deprotonated neutral fluorophore was located in the micelle.[36] This partitioning of the acid and base in the ground state led to colour changes for the emission from the gel with changes in pH and temperature. In both cases white light emission was achieved for defined experimental conditions, but in the BTS/F127 gel temperature and pH did not trigger a change in colour. These examples show that depending on the properties desired for an emissive material, the design of the fluorophore requires tuning of photophysical and structural properties to target the desired location of the fluorophore within the compartments of the supramolecular system.

Conclusions

Our supramolecular strategy showed that microheterogeneous systems can segregate non-soluble fluorophores. Micelles in the sol and gel phases are examples of such microheterogeneous systems where molecules are incorporated into specific environments of the system depending on the properties of each environment. In the present case, a luminescent material was prepared by designing the photophysical and structural properties of the fluorophore. The aqueous insolubility of BTS led to its incorporation only in the F127 micellar core without a partitioning of BTS molecules between the micellar core and corona. Such a partitioning occurs for less hydrophobic fluorophores. The specific localization of BTS is responsible for the complete protection of the fluorophore from changes in pH in the hydrogel, leading to a material where its emissive properties will not depend on the pH of the surrounding environment. The broad emission spectrum observed for the BTS/F127 gel ensured that white light emission was observed at the lower BTS concentrations, showing that the micellar environment avoids the formation of BTS aggregates which would alter the colour of the gel's emission. The environmental control of the photophysical properties of BTS in the F127 gel is of relevance for the development of materials for applications, such as biosensing, imaging, and display technologies where exposure to water at different pHs is possible but a change in the emission colour of the material because of these different pHs is undesirable.

Author contributions

Ankur A. Awasthi: investigation, methodology development, data analysis and writing. Luís Gustavo Teixeira Alves Duarte: conceptualization, formal analysis, writing, review and editing. Fabiano Severo Rodembusch: funding acquisition, supervision, review and editing. Teresa Dib Zambon Atvars: funding

acquisition, review and editing. Cornelia Bohne: funding acquisition, conceptualization, supervision, writing, review and editing.

Conflicts of interest

There are no conflicts to declare.

Data availability

The data supporting this article have been included as part of the supplementary information (SI). Supplementary information: ^{1}H NMR spectra of BTS, emission spectra of BTS/F127 gels, chromaticity diagrams and coefficients for the emission of BTS in F127 hydrogels, time-resolved fluorescence of BTS/F127 gels. See DOI: https://doi.org/10.1039/d5sm00788g.

Acknowledgements

References

1 B. Blanco-Fernandez, V. M. Gaspar, E. Engel and J. F. Mano, Proteinaceous Hydrogels for Bioengineering Advanced 3D Tumor Models, *Adv. Sci.*, 2021, **8**, 2003129.

2 S. Mitura, A. Sionkowska and A. Jaiswal, Biopolymers for Hydrogels in Cosmetics: Review, *J. Mater. Sci.: Mater. Med.*, 2020, **31**, 50.

3 M. Wang, Y. Cheng, X. Li, L. Nian, B. Yuan, S. Cheng, S. Wang and C. Cao, Effects of Microgels Fabricated by Microfluidic on the Stability, Antioxidant, and Immunoenhancing Activities of Aquatic Protein, *J. Future Foods*, 2025, **5**, 57–67.

4 A. C. Barbati, J. Desroches, A. Robission and G. H. McKinley, Complex Fluids and Hydraulic Fracturing, *Annu. Rev. Chem. Biomol. Eng.*, 2016, **7**, 415–453.

5 Y. Bai, S. He, Y. Lian, T. Yu, C. Dai, J. Zhao and H. Zhang, Self-Lubricating Supramolecular Hydrogel for In-Depth Profile Control in Fractured Reservoirs, *ACS Omega*, 2020, **5**, 7244–7253.

6 Y. S. Zhang and A. Khademhosseini, Advances in Engineering Hydrogels, *Science*, 2017, **356**, eaaf3627.

7 H. Abdeltawab, D. Svirskis and M. Sharma, Formulation Strategies to Modulate Drug Release from Poloxamer Based In Situ Gelling Systems, *Expert Opin. Drug Delivery*, 2020, **17**, 495–509.

8 R. Malečková, Š. Tumová, P. Smísitel, J. Smilek, H. Šimůnková, M. Pešková, L. Kubáč, J. Hubálek, J. Víteček, M. Vala and M. Weiter, Novel Conductive PEDOT:DBSA Hydrogels with Tuneable Properties for Bioelectronics, *Mater. Adv.*, 2025, **6**, 1278–1287.

9 Y. Wei, J. Tang, J. Zhang, Y. Lin and C. Zheng, A Label-free Fluorescent-hydrogel Sensor for Heparin Detection in Diluted Whole Blood, *Chem. Commun.*, 2025, **61**, 1215–1218.

10 K. V. Rao, K. Jayaramulu, T. K. Maji and S. J. George, Supramolecular Hydrogels and High-Aspect-Ratio Nanofibers through Charge-Transfer-Induced Alternate Coassembly, *Angew. Chem., Int. Ed.*, 2010, **49**, 4218–4222.

11 A. A. Sagade, K. V. Rao, U. Mogera, S. J. George, A. Datta and G. U. Kulkarni, High-Mobility Field Effect Transistors Based on Supramolecular Charge Transfer Nanofibres, *Adv. Mater.*, 2013, **25**, 559–564.

12 A. S. Weingarten, R. V. Kazantsev, L. C. Palmer, M. McClendon, A. R. Koltonow, A. P. S. Samuel, D. J. Kiebala, M. R. Wasielewski and S. I. Stupp, Self-assembling Hydrogel Scaffolds For Photocatalytic Hydrogen Production, *Nat. Chem.*, 2014, **6**, 964–970.

13 A. S. Weingarten, R. V. Kazantsev, L. C. Palmer, D. J. Fairfield, A. R. Koltonow and S. I. Stupp, Supramolecular Packing Controls H_2 Photocatalysis in Chromophore Amphiphile Hydrogels, *J. Am. Chem. Soc.*, 2015, **137**, 15241–15246.

14 S. Wei, Z. Li, W. Lu, H. Liu, J. Zhang, T. Chen and B. Z. Tang, Multicolor Fluorescent Polymeric Hydrogels, *Angew. Chem.*, 2021, **133**, 8690–8706.

15 S. Liao, Z. Li, L. Ren, T. Lin, C. Lin, C. Zhao, M. Gao and X. Wu, Multicolor Tunable AIE Fluorescent Hydrogels Containing Europium Ionic Complexes via the "One-Pot Method", *ACS Appl. Polym. Mater.*, 2025, **7**, 700–709.

16 J. Huang, Y. Ma, X. Jiang, J. Xian, Z. Fu and H. Ouyang, Robust Luminescent Pyrene-Based Metal−Organic Framework Hydrogel as a pH-Responsive Fluorescence Emitter for Sensitive Immunoassay of Cardiac Troponin I, *Anal. Chem.*, 2024, **86**, 15042–15049.

17 J. Ding and C. V. Kumar, Non-covalent Assembly of Multiple Fluorophores in Edible Protein/Lipid Hydrogels for Applications in Multi-step Light Harvesting and White-light Emission, *Molecules*, 2023, **28**, 6028.

18 S. M. Shet, M. Bisht, S. Pramanik, S. Roy, T. S. Kumar, S. K. Nataraj, D. Mondal and S. Bhandari, Engineering Quantum Dots with Ionic Liquid: A Multifunctional White Light Emitting Hydrogel for Enzyme Packaging, *Adv. Opt. Mater.*, 2020, 1902022.

19 M. Li, P. He, S. Li, X. Wang, L. Liu, F. Lv and S. Wang, Oligo(p-phenylenevinylene) Derivative-Incorporated and Enzyme-Responsive Hybrid Hydrogel for Tumor Cell-Specific Imaging and Activatable Photodynamic Therapy, *ACS Biomater. Sci. Eng.*, 2018, **4**, 2037–2045.

20 Y.-H. Tsou, X.-Q. Zhang, X. Bai, H. Zhu, Z. Li, Y. Liu, J. Shi and X. Xu, Dopant-Free Hydrogels with Intrinsic Photoluminescence and Biodegradable Properties, *Adv. Funct. Mater.*, 2018, **28**, 1802607.

21 X.-J. Wang, H.-L. Mo, C.-W. Wei, S.-Q. Gao and Y.-W. Lin, White-light-emitting Ln-hydrogels with Multi-stimuli Responsiveness and Applications in Environmental Sensing and Anti-counterfeiting, *Phys. Chem. Chem. Phys.*, 2023, **25**, 18354–18363.

22 W. Mróz, G. Tullii, E. Kozma and F. Galeotti, Harnessing Perylene Emitters in Soft Hydrogels for White Light Generation, *ACS Appl. Opt. Mater.*, 2024, **2**, 2380–2386.

23 S. S. Babu, V. K. Praveen and A. Ajayaghosh, Functional π-Gelators and Their Applications, *Chem. Rev.*, 2014, **114**, 1973–2129.

24 Q. Ma, D. Kong, X. Min, X. Yu, P. Yan, Y. Han, Q. Tian and H. Lv, Supramolecular Luminescent Hydrogel Based on Glycine/Terbium Complex and Fluorescent Dyes for Visual Temperature Monitoring, *Adv. Opt. Mater.*, 2025, **13**, 2402077.

25 K. Benson, A. Ghimire, A. Pattammattel and C. V. Kumar, Protein Biophosphors: Biodegradable, Multifunctional, Protein-Based Hydrogel for White Emission, Sensing, and pH Detection, *Adv. Funct. Mater.*, 2017, **27**, 1702955.

26 Z. Zhang, D. Wang, X. Yan, Y. Yan, L. Lin, Y. Ren, Y. Chen and L. Feng, Efficient Chiral Hydrogel Template Based on Supramolecular Self-assembly Driven by Chiral Carbon Dots for Circularly Polarized Luminescence, *J. Colloid Interface Sci.*, 2024, **674**, 576–586.

27 L. Zhang, S. R. Jean, S. Ahmed, P. M. Aldridge, X. Li, F. Fan, E. H. Sargent and S. O. Kelley, Multifunctional Quantum Dot DNA Hydrogels, *Nat. Commun.*, 2017, **29**, 381.

28 J. Zhang, J. Jin, J. Wan, S. Jiang, Y. Wu, W. Wang, X. Gong and H. Wang, Quantum Dots-based Hydrogels for Sensing Applications, *Chem. Eng. J.*, 2021, **408**, 127351.

29 A. Cayuela, M. L. Soriano, S. R. Kennedy, J. W. Steed and M. Valcárcel, Fluorescent Carbon Quantum Dot Hydrogels for Direct Determination of Silver Ions, *Talanta*, 2016, **151**, 100–105.

30 M. Li, P. Zhang, J. Mao, J. Li, Y. Zhang, B. Xu, J. Zhou, Q. Cao and H. Xiao, Construction of Cellulose-based Hybrid Hydrogel Beads Containing Carbon Dots and Their High Performance in the Adsorption and Detection of Mercury Ions in Water, *J. Environ. Manage.*, 2024, **359**, 121076.

31 Y. Liu, J. Jiang, X. Huang, J. Tang, Q. Tan, Y. Chen, Y. Xiao, X. Wu and G. Weng, Reversible White-Light-Driven Photochromic Polymer Hydrogels with High Stretchability and Adhesiveness, *ACS Appl. Polym. Mater.*, 2023, **5**, 8207–8215.

32 Q. Zhu, L. Zhang, K. V. Vliet, A. Miserez and N. Holten-Anderson, White Light-Emitting Multi-Stimuli-Responsive Hydrogel with Lanthanides and Carbon Dots, *ACS Appl. Mater. Interfaces*, 2018, **10**, 10409–10418.

33 K. Janani Archana and K. Balasubramanian, Tandem FRET: A Robust Mechanism for Efficient Fabrication of WLED Using an Organic–Inorganic Hybrid Mixture, *ACS Appl. Opt. Mater.*, 2024, **2**, 885–895.

34 J. M. Galindo, J. Leganés, J. Patiño, A. M. Rodríguez, M. A. Herrero, E. Díez-Barra, S. Merino, A. M. Sánchez-Migallón and E. Vázquez, Physically Cross-Linked Hydrogel Based on Phenyl-1,3,5-triazine: Soft Scaffold with Aggregation-Induced Emission, *ACS Macro Lett.*, 2019, **8**, 1391–1395.

35 Z. Li, P. Liu, X. Ji, J. Gong, Y. Hu, W. Wu, X. Wang, H.-Q. Peng, R. T. K. Kwok, J. W. Y. Lam, J. Lu and B. Z. Tang, Bioinspired Simultaneous Changes in Fluorescence Color, Brightness, and Shape of Hydrogels Enabled by AIEgens, *Adv. Mater.*, 2020, **32**, 190649.

36 J. Wang, F. Tang, Y. Wang, S. Liu and L. Li, Tunable Single-Molecule White-Light Emission in Stimuli-Responsive Hydrogel, *Adv. Opt. Mater.*, 2020, **8**, 1901571.

37 C. N. Zhu, T. Bai, H. Wang, W. Bai, J. Ling, J. Z. Sun, F. Huang, Z. L. Wu and Q. Zheng, Single Chromophore-Based White-Light-Emitting Hydrogel with Tunable Fluorescence and Patternability, *ACS Appl. Mater. Interfaces*, 2018, **10**, 39343–39352.

38 S. S. Thomas, H. Hosseini-Nejad and C. Bohne, Dynamics of Small Molecules within the F127 PEO–PPO–PEO Triblock Copolymer Gel and Sol Phases Studied at the Molecular Scale, *Soft Matter*, 2022, **18**, 1706–1714.

39 C. Bohne, Supramolecular Dynamics, *Chem. Soc. Rev.*, 2014, **43**, 4037–4050.

40 L. G. T. A. Duarte, J. C. Germino, J. F. Berbigier, C. A. Barboza, M. M. Faleiros, D. de Alancar Simoni, M. T. Galante, M. S. de Holanda, F. S. Rodembusch and T. D. Z. Atvars, White-light Generation from All-solution-processed OLEDs using a Benzothiazole–salophen Derivative Reactive to the ESIPT Process, *Phys. Chem. Chem. Phys.*, 2019, **21**, 1172–1182.

41 E. M. Kosower and D. Huppert, Excited State Electron and Proton Transfers, *Annu. Rev. Phys. Chem.*, 1986, **37**, 127–156.

42 T. Förster, Diabatic and Adiabatic Processes in Photochemistry, *Pure Appl. Chem.*, 1970, **24**, 443–450.

43 L. G. T. A. Duarte, E. S. Moraes, P. S. S. Wakabayashi, L. C. da Luz, R. Cercená, E. Zapp, T. D. Z. Atvars, A. G. Dal-Bó and F. S. Rodembusch, Revealing the ESIPT process in benzoxazole fluorophores within polymeric matrices through theory and experiment, *Photochem. Photobiol.*, 2025, **101**, 290–301.

44 E. Stoekler, G. Ulrich, P. Retailleau, A. D. Laurent, D. Jaquemin and J. Massue, Experimental and theoretical comprehension of ESIPT fluorophores based on a 2-(20-hydroxyphenyl)-3,30-dimethylindole (HDMI) scaffold, *Chem. Sci.*, 2024, **15**, 7206–7218.

45 L. G. T. A. Duarte, J. C. Germino, R. A. Mendes, J. F. Berbigier, M. M. Faleiros, F. S. Rodembusch and T. D. Z. Atvars, The Role of a Simple and Effective Salicylidene Derivative. Spectral Broadening and Performance Improvement of PFO-based all-solution Processed OLEDs, *Dye Pigment*, 2019, **171**, 107671.

46 L. G. T. A. Duarte, J. C. Germino, R. A. Mendes, J. F. Berbigier, K. S. Moreira, M. M. Faleiros, J. N. de Freitas, T. A. L. Burgo, F. S. Rodembusch and T. D. Z. Atvars, The Balance between Charge Mobility and Efficiency in All-Solution-Processed Organic Light-Emitting Diodes of Zn(II) Coordination Compounds/PFO Composites, *J. Phys. Chem. C*, 2020, **124**, 21036–21046.

47 P. Alexandridis, J. F. Holzwarth and T. A. Hatton, Micellization of Poly(ethylene oxide)-Poly(propylene oxide)-Poly(ethylene oxide) Triblock Copolymers in Aqueous Solutions: Thermodynamics of Copolymer Association, *Macromolecules*, 1994, **27**, 2414–2425.

48 Z. Tuzar and P. Kratochvíl, Block and Graft Copolymer Micelles in Solution, *Macromolecules*, 1994, **6**, 201–232.

49 J. J. Escobar-Chávez, M. López-Cervantes, A. Naïk, Y. N. Kalia, D. Quintanar-Guerrero and A. Ganem-Quintanar, Applications of Thermo-reversible Pluronic F-127 Gels in Pharmaceutical Formulations, *J. Pharm. Pharm. Sci.*, 2006, **9**, 339–358.

50 Y. Shiraishi, T. Inoue and T. Hirai, Local Viscosity Analysis of Triblock Copolymer Micelle with Cyanine Dyes as a Fluorescent Probe, *Langmuir*, 2010, **26**, 17505–17512.

51 U. Anand and S. Mukherjee, Microheterogeneity and Microviscosity of F127 Micelle: The Counter Effects of Urea and Temperature, *Langmuir*, 2014, **30**, 1012–1021.

52 R. Basak and R. Bandyopadhyay, Encapsulation of Hydrophobic Drugs in Pluronic F127 Micelles: Effects of Drug Hydrophobicity, Solution Temperature, and pH, *Langmuir*, 2013, **29**, 4350–4356.

53 C. Bohne, R. W. Redmond and J. C. Scaiano, *Photochemistry in Organized and Constraint Media*, ed. V. Ramamurthy, VCH Publishers, New York, 1991, pp. 79–132.

54 D. Zhang, X. Liu, Y. Yin, Z. Chen, W. M. J. Han and Y. Yang, Theoretical Insights on the Double ESIPT Mechanism and Fluorescence Properties of H2BIo Chromophore, *Spectrochim. Acta, Part A*, 2025, **331**, 125795.

55 K. L. Kelly, Color Designations for Lights, *J. Opt. Soc. Am.*, 1943, **33**, 627–632.

56 L. G. T. A. Duarte, F. S. Rodembusch, T. D. Z. Atvars and R. G. Weiss, Experimental and Theoretical Investigation of Excited-State Intramolecular Proton Transfer Processes of Benzothiazole Derivatives in Amino-polydimethylsiloxanes before and after Cross- Linking by CO_2, *J. Phys. Chem. A*, 2020, **124**, 288–299.

57 D. P. Chatterjee, M. Pakhira and A. K. Nandi, Fluorescence in "Nonfluorescent" Polymers, *ACS Omega*, 2020, **5**, 30747–30765.

58 A. S. R. Koti, M. M. G. Krishna and N. Periasamy, Time-Resolved Area-Normalized Emission Spectroscopy (TRANES): A Novel Method for Confirming Emission from Two Excited States, *J. Phys. Chem. A*, 2001, **105**, 1767–1771.

59 A. S. R. Koti and N. Pariasamy, Application of Time Resolved Area Normalized Emission Spectroscopy to Multicomponent Systems, *J. Chem. Phys.*, 2001, **115**, 7094–7099.

60 J. Cheng, K. Wei, X. Ma, X. Zhou and H. Xiang, Synthesis and Photophysical Properties of Colorful Salen-Type Schiff Bases, *J. Phys. Chem. C*, 2013, **117**, 16552–16563.

61 M. G. Vivas, J. C. Germino, C. A. Barboza, D. D. A. Simoni, P. A. M. Vazquez, L. De Boni, T. D. Z. Atvars and C. R. Mendonça, Revealing the Dynamic of Excited State Proton Transfer of a π-Conjugated Salicylidene Compound: An Experimental and Theoretical Study, *J. Phys. Chem. C*, 2017, **121**, 1283–1290.

62 T. Khan and A. Datta, Impact of Molecular Arrangement and Torsional Motion on the Fluorescence of Salophen and Its Metal Complexes, *J. Phys. Chem. C*, 2017, **121**, 2410–2417.